J. Ind. Geophys. Union, 29(6) (2025), 394-399

Comparison of seismic displacement, velocity and acceleration for discriminating landslides from earthquakes and background noise

Mahesh Yezarla[1, 2], Rajesh Rekapalli[1, 2*], Raviteja Kethavarapu[1]
[1] CSIR-National Geophysical Research Institute, Hyderabad- 500007, India
[2] Academy of Scientific and Innovative Research (AcSIR), Ghaziabad- 201002, India
*Corresponding author: rekapalli@gmail.com

ABSTRACT

Seismic signals from landslides, earthquakes, and background noise exhibit distinct spectral characteristics that enable effective event classification. This study presents a comparison of the Power Spectral Density (PSD) of seismic displacement, velocity, and acceleration. We analyzed frequency power distribution and power decay rates using PSDs, estimated from all three ground motion measurements. The seismic displacement signals of landslides are characterized by gradual amplitude evolution and dominant low-frequency content, whereas earthquakes show impulsive energy release with broader frequency bandwidths. Our results demonstrate that the landslides exhibit distinct spectral trends that are more pronounced in the PSD of acceleration data, compared to earthquake and ambient noise. Additionally, background noise displays a more stable and less structured spectral profile. Furthermore, we have achieved 98% accuracy in the detection of landslides using PSD features from displacement, velocity, and acceleration domains when using a frequency range of 1–10 Hz. The study suggests that the analysis of seismic waveform PSD is a robust and region-independent method for seismic event characterization, particularly for rapid landslide detection and geohazard monitoring.

Keywords: Landslide, Earthquake, Acceleration, Velocity, Displacement, Power Spectral Density

INTRODUCTION

Seismic monitoring plays a crucial role in identifying and characterizing geohazard events such as earthquakes and landslides. Seismic monitoring of slope failures began way back in the late 1960s (Cadman and Goodman 1967; Novosad et al., 1977), and has evolved to a mature state at present to think of a seismic early warning system for slope failures and associated mass movements (Cook et al., 2021; Rao et al., 2021). While both earthquakes and landslides generate seismic waves, their distinct source mechanisms result in different spectral properties. Landslides involve the progressive downslope movement of mass, leading to prolonged and evolving seismic signals. In contrast, earthquakes are characterized by sudden fault rupture, generating impulsive energy over a broad frequency range. Differentiating these events from background seismic noise is essential for accurate event classification in the early warning systems. The analysis of seismic signal spectral powers facilitates understanding the differences (Suriñach et al., 2005; Chen et al., 2014; Burtin et al., 2014; Cook et al., 2021; Rao et al., 2021; Rekapalli et al., 2024). Surinach et al., (2005) have analyzed the seismic waveforms of landslides in comparison with those of earthquakes and found support for their hypothesis that "increase in the frequencies and amplitudes with time in the spectrograms is associated with the mass movements on the surface". Based on the spectral characteristics, Rekapalli et al. (2024) have developed a global spectral model for discriminating seismic signals of landslides from earthquakes and noise, using PSDs of seismic velocity waveforms. They have successfully demonstrated the robustness of the method on a data set of ~835 landslide waveforms from different regions of the globe. As an extension to Rekapalli et al. (2024), this study focuses on providing a comparative analysis of the spectral models of seismic displacement, velocity and acceleration waveforms of landslides, earthquakes and noise data to compare their distinct power decay rates for discriminating landslides from the other two classes in real-time.

DATA AND METHODOLOGY

The study uses the seismic waveforms downloaded from the FDSN data portal (https://www.fdsn.org/networks/). We have identified nearly 28 landslides over the globe and downloaded corresponding data available from AK (Alaska Earthquake Center, Univ. of Alaska Fairbanks,1987), CH (Swiss Seismological Service, SED at ETH Zurich, 1983), CN (Natural Resources Canada,1975), GE (GEOFON Data Centre, 1993). IU (Albuquerque Seismological Laboratory/ USGS, 2014) and TW (Institute of Earth Sciences, Academia Sinica, Taiwan, 1996) networks through the portal. We have also downloaded an equal number of small magnitude earthquake waveforms that were recorded by the same networks and occurred in the vicinity of the landslide locations, keeping the same events (landslide, earthquake) to station distance. Similarly, we collected noise recorded before the landslide from the same recording station to prepare the same number of noise data sets. We prepared data of three labelled classes (landslide, earthquakes and noise waveforms). The waveform duration was fixed at 300 seconds in each class. As the minimum sampling rate of some seismic recordings is 20 samples/ second, all the data were resampled to 20 samples per second. All three data sets were corrected for instrument response using the station XML files in Obspy (Beyreuther et al., 2010) and converted to respective displacement, velocity and acceleration waveforms. In this study, we estimated the power spectral density (PSD) of the seismic waveforms using the Fourier transform-based Welch's periodogram method.

The PSDs were computed using NFFT=1024 with 50 % overlap using the ObsPy library in Python.

ANALYSIS AND RESULTS

In the first step, 912 seismic waveforms of 28 landslides, 1011 signals of 28 earthquakes, and 1065 noise signals adjacent to landslide signals were downloaded from the FDSN server to develop the mean PSD models of seismic displacement, velocity, and acceleration. We considered small magnitude earthquakes with recording station distances nearly equal to those of the corresponding landslides. As these waveforms were collected from different parts of the globe/ diverse geological environments, the mean PSD models from this data represent the global or generalized model for the particular process and therefore help to examine the spectral characteristics of landslide, earthquake, and noise signals for their detection. Figure 1 shows the mean PSD models derived from the seismic displacement, velocity and acceleration signals associated with landslide, earthquake and noise processes.

From Figure 1, it can be noticed that the PSDs of landslide, earthquake and noise, computed from the three seismic measurements (displacement, velocity and acceleration) are separable. However, separability is minimum for the displacement data and maximum for the acceleration data. The PSDs of acceleration data show clear distinctions because earthquakes typically carry strong energy in higher frequencies (1–10 Hz) from sharp and impulsive wave arrivals, while landslides produce comparatively lower-frequency signals due to slower, mass-driven movements.

Further, we have also compared the mean PSDs computed from different regions to see the consistency in the trend of the PSD. Figure 2 shows the mean PSDs of Alaska (3 events, 92 traces), Utah (2 events, 155 traces), Switzerland (2 events, 8 traces), Mount Meager in British Columbia (1 event, 57 traces), and China (1 event, 11 traces) regions. Despite differences in tectonic settings, topography, and the number of records, the PSD decay trend remains consistent across all the regions. Each region exhibits high power in the 0.01 to 5 Hz frequency band. These models corroborated well with the global model given in Rekapalli et al. (2024). We can also notice the consistency in the PSDs of displacement, velocity, and acceleration data from different regions. This consistent decay pattern demonstrates that the PSD characteristics of seismic recordings of landslide signals are strongly governed by the underlying landslide dynamics. This strengthens the generality of our approach and suggests that PSD-based features can be applied robustly across global datasets.

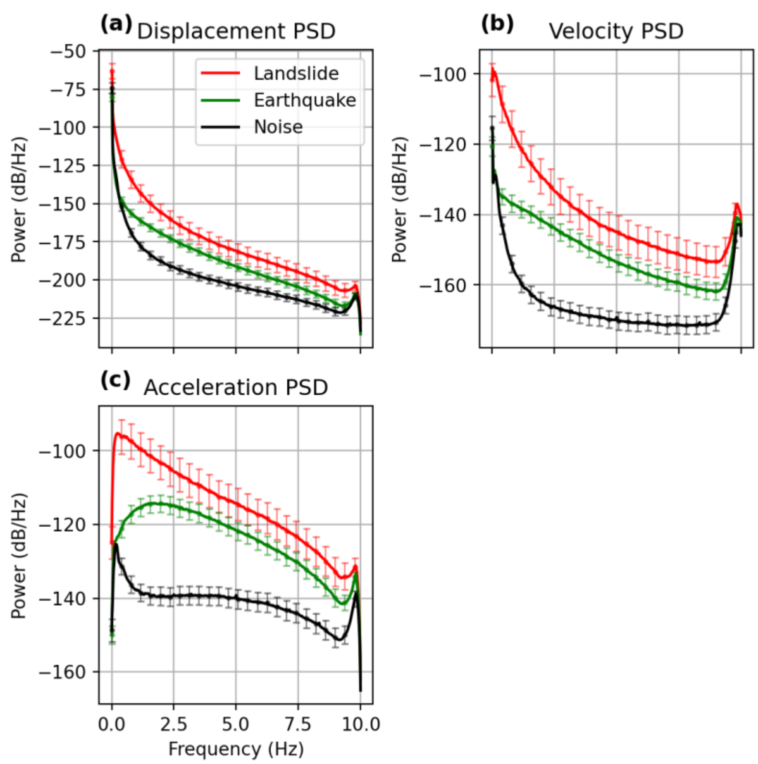

Figure 1. A comparison of mean global PSDs of landslide, earthquake and noise processes computed using the Welch's periodogram method from seismic **(a)** displacement, **(b)** velocity and **(c)** acceleration measurements, corresponding to 28 landslides, 28 comparable small magnitude earthquakes and background noise chunks collected before/ after the landslide events, along with standard errors.

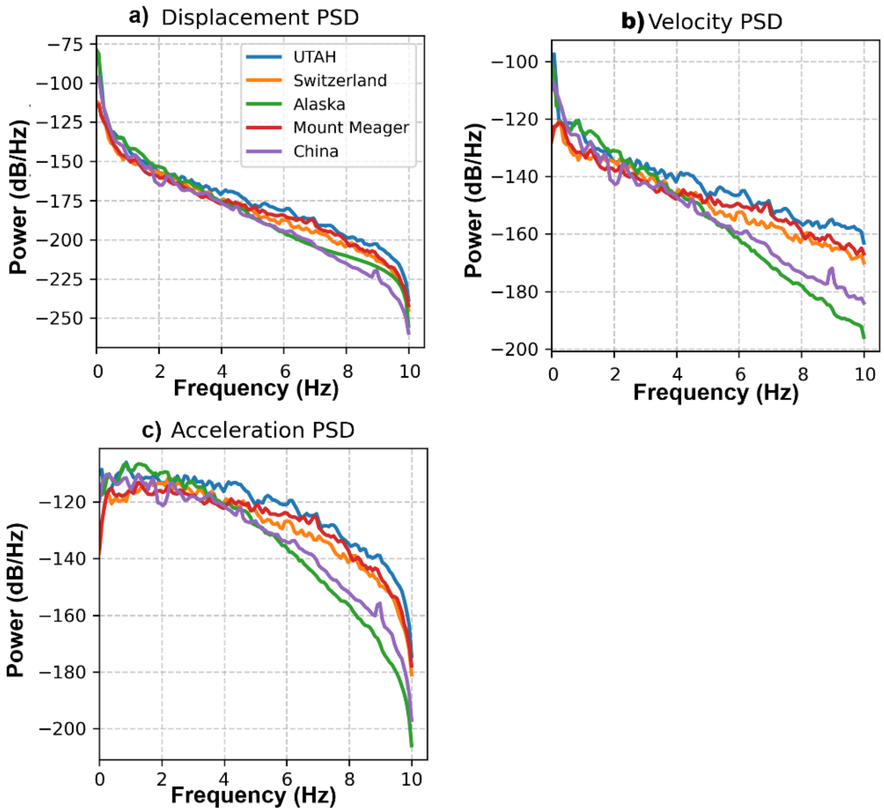

Figure 2. A comparison of mean PSD of landslides computed from seismic **(a)** displacement, **(b)** velocity and **(c)** acceleration measurements from Alaska (3 events, 92 traces), Utah (2 events, 155 traces), Switzerland (2 events, 8 traces), Mount Meager in British Columbia (1 event, 57 traces), and China (1 event, 11 traces).

Finally, we tested this approach on the seismic signals recorded at station TWGB (Network: TW), located at 22.82° N and 121.08 ° E, in Taiwan, after the Mw 7.4 Hualien earthquake that occurred on 3rd April 2024. The waveforms of a small magnitude aftershock occurred on 2024-04-03 between 01:54:00 and 01:56:30 UTC and the landslide that occurred between 00:11:00 and 00:16:00 UTC on 2024-04-03 following the April 3, 2024, Mw 7.4 Hualien earthquake, were used in the study for testing the global spectral models of seismic displacement, velocity and acceleration for landslide detection. The noise data was taken from a 5-minute window before the landslide event, with a start time of 2024-04-03T00:06:00 and an end time of 2024-04-03T00:11:00. It represents background seismic activity at station TWGB and serve as a reference for distinguishing landslide and earthquake signals from ambient noise. The raw data of landslides, earthquakes, and noise converted to displacement, velocity, and acceleration are shown in Figure 3. Figure 4 shows the PSDs of three processes from the TWGB station estimated from three domains. We can observe that the PSDs of earthquake, landslide and noise are clearly separable when using the PSDs of seismic velocity and acceleration measurements, whereas the separability is poor for PSDs computed from seismic displacements (Figure 4).

Random Forest classification of seismic events using Multi-Domain Spectral Features

Here, we analyze the frequency dependency of the classification performance of seismic signals associated with landslides, earthquakes, and noise by using ground displacement, velocity, and acceleration measurements together. We used the Power Spectral Density (PSD) features extracted in all three domains to capture distinct spectral characteristics of each event type. In total, 8964 PSDs were analyzed (landslides: 2736, earthquakes: 3033, and noise: 3195), with each event represented in three domains (displacement, velocity, and acceleration). A Random Forest classifier was trained and evaluated using a 70-30 train-test split. We systematically varied the lower cutoff frequency of the bandpass filter using 10 Hz as the fixed upper cutoff to assess the influence of frequency band selection on classification performance. The accuracies of the classification model at different low-frequency cut-offs are shown in Table 1. The model achieved 95% accuracy when using a frequency range of 0.001–10 Hz. Increasing the lower cutoff to 0.01 Hz has improved accuracy to 96% and 98% accuracy was noticed when increasing the lower cutoff frequencies to 0.1 Hz and 1 Hz.

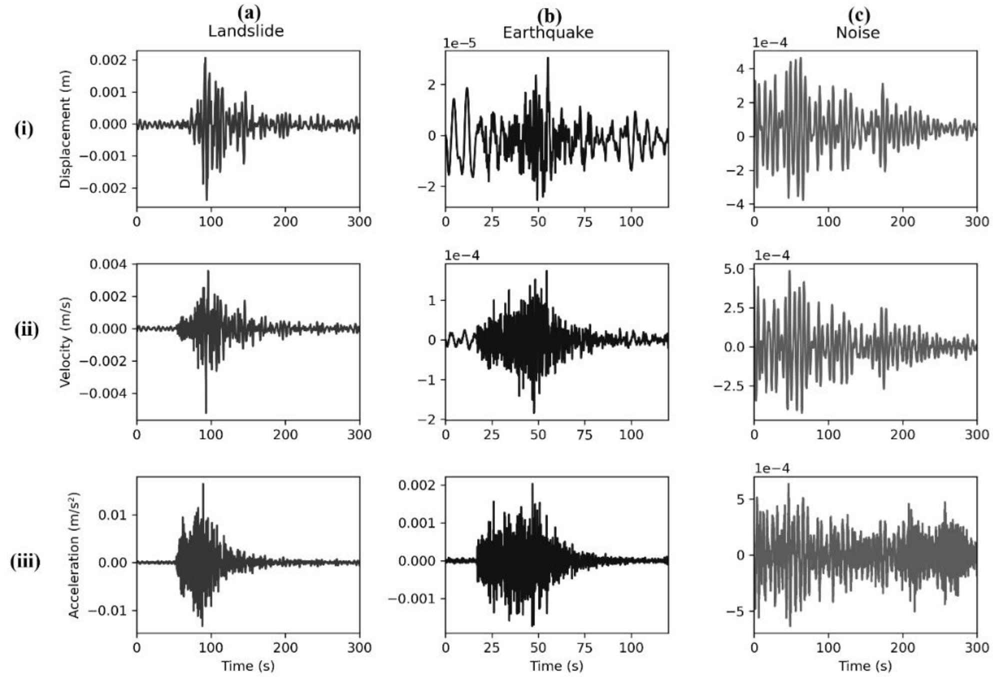

Figure 3. Seismic **(i)** displacement **(ii)** velocity and **(iii)** acceleration waveforms of **(a)** landslide **(b)** earthquake and **(c)** background noise recorded on 3rd April 2024 at the TWGB station after the Taiwan earthquake.

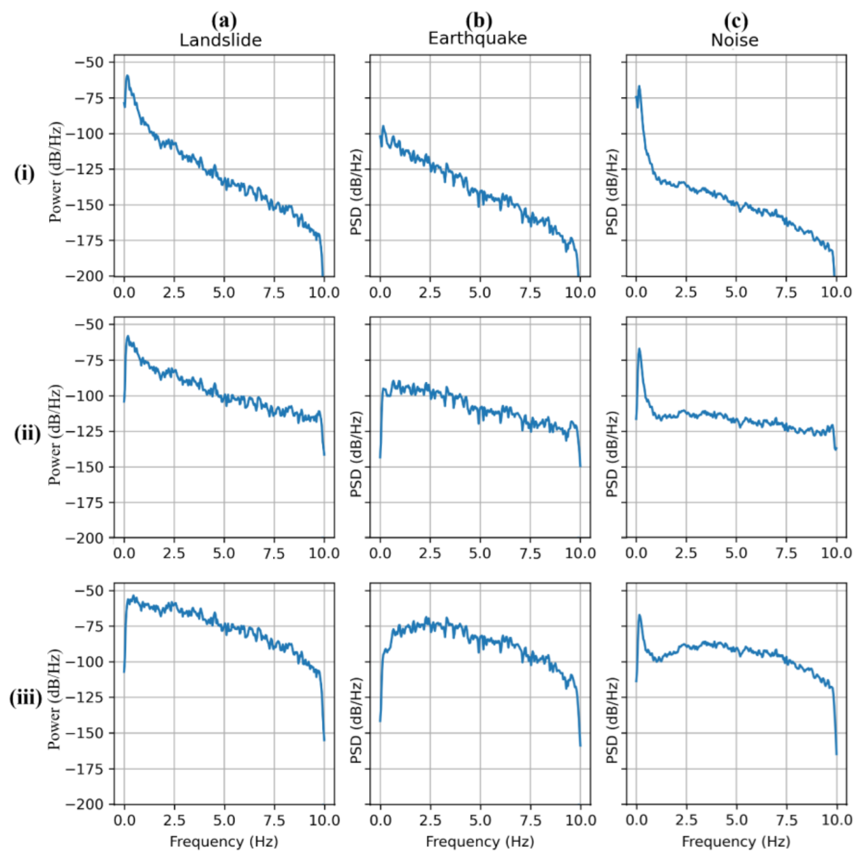

Figure 4. PSDs of seismic **(i)** displacement **(ii)** velocity and **(iii)** acceleration waveforms of **(a)** landslide **(b)** earthquake and **(c)** background noise recorded on 3rd April 2024 at the TWGB station after the Taiwan earthquake.

Table 1. The classification accuracy of the random forest model when using PSD attributes of seismic waveforms (displacement, velocity and acceleration) at different lower cutoff frequencies.

Lower cutoff frequency (Hz)	Upper cutoff frequency (Hz)	Accuracy (%)
0.001	10	95.0
0.01	10	96.0
0.1	10	98.0
1	10	98.0

The accuracy attained with the PSDs of seismic displacement, velocity and acceleration together as input is slightly higher than the accuracy obtained from individual displacement (97%) and acceleration (97%) and is almost equal to the accuracy achieved using velocity data (98%) when using the frequency band 0.01 to 10 Hz.

These results indicate that the optimal frequency selection and usage of all three ground motion measurements (displacement, velocity, and acceleration), significantly enhances feature diversity and that optimal selection of frequency bands during preprocessing plays a crucial role in classification performance. The improved results at higher frequency thresholds suggest that very low-frequency components may introduce noise or baseline drift, which can obscure class-specific spectral features. Conversely, mid- to high-frequency content appears to hold the most discriminative information for distinguishing landslides from earthquakes and noise. Thus, our results demonstrate the effectiveness of PSD-based analysis in seismic signal classification and provide a foundation for optimizing processing parameters, which would be useful for real-time geo hazard monitoring systems.

DISCUSSION AND CONCLUSIONS

Recent advancements in the seismic network-based monitoring of non-earthquake geohazards (Diaz et al., 2014; Burtin et al., 2016; Hürlimann et al., 2019; Cook and Dietze, 2022) have gained increasing attention due to their customizable spatiotemporal resolution and ability to detect hazardous events remotely. These features help to overcome the limitations of satellite and in-situ approaches in terms of coverage and accessibility. Although, these methods have been robustly tested across diverse geographic regions, their real-time utility for early warning systems has not been explored due to the difficulties in the detection and discrimination of seismic signals and their sources. In Particular, identifying landslide-generated seismic signals from earthquakes and local noise signals has been a challenge due to unclear phases and low SNR.

Rekapalli et al. (2024) proposed a robust and simple approach by analyzing PSDs of ~835 seismic velocity waveforms from 28 global landslides, alongside an equal number of small-magnitude earthquakes and noise signals and their skewness. The study has shown that PSDs of 95.82% of landslide seismic velocity waveforms correlate with a correlation coefficient above 0.6 with the global mean PSD model. Building upon this work, the present study focuses on computing and comparing the PSD models of seismic displacement and acceleration with the results obtained from seismic velocity waveforms. We extended the global data set used by Rekapalli et al. (2024) with nearly 912 landslide, earthquake and noise waveforms for computing the global PSD models. We tested the models using continuous seismic waveforms with landslide, earthquake and noise signals recorded at the TWGB station in Taiwan on 3rd April 2024, after the 2nd April 2024 Taiwan earthquake. The distinction between landslide signals and other sources is clear in the PSDs derived from velocity and acceleration, compared to those from displacement data. Therefore, we recommend using either seismic velocity or acceleration data for landslide monitoring applications, as they offer superior discriminative power over displacement data.

Additionally, our machine learning classification results show that incorporating PSD features from all three ground motion measurements can increase accuracy as high as 98%. In addition, the accuracy of ML models using individual velocity and acceleration measurements is also ~98% when the analysis is limited to the 1–10 Hz frequency band. This underscores the critical role of both domain selection and targeted frequency filtering in improving the precision of seismic landslide detection.

Acknowledgments

We thank the Director, CSIR-NGRI, Hyderabad for his kind permission to publish this work (NGRI/Lib/2025/Pub-110). We acknowledge the FDSN data portal (https://www.fdsn.org/networks/) for the waveform data from global seismic networks.

Author Credit Statement

Mahesh Yazarla: Data collection, methodology, formal analysis and writing the original draft and edits. Rajesh Rekapalli: Conceptualization, methodology, formal analysis, interpretation and writing the original draft and edits. K.

Raviteja: Data collection, methodology, formal analysis, and writing the original draft and edits.

Data Availability

The data used in the study can be downloaded from FDSN data portal (https://www.fdsn.org/networks/).

Compliance with Ethical Standards

The authors declare no conflict of interest and adhere to copyright norms.

REFERENCES

Beyreuther, M., Barsch, R., Krischer, L., Megies, T., Behr, Y. and Wassermann, J., 2010. ObsPy: A Python toolbox for seismology. Seismological Res. Lett., 81(3), 530-533.

Burtin, A., Hovius, N. and Turowski, J.M., 2014. Seismic monitoring of geomorphic processes. Earth Surface Dynamics, 2(2), 1217-1267.

Burtin, A., Hovius, N. and Turowski, J.M., 2016. Seismic monitoring of torrential and fluvial processes. Earth Surface Dynamics, 4(2), 285-307.

Cadman, J.D. and Goodman, R.E., 1967. Landslide noise. Science, 158(3805), 1182-1184.

Chen, T.C., Lin, M.L. and Wang, K.L., 2014. Landslide seismic signal recognition and mobility for an earthquake-induced rockslide in Tsaoling, Taiwan. Engineering Geol., 171, 31-44.

Cook, K.L. and Dietze, M., 2022. Seismic advances in process geomorphology. Ann. Review Earth Planet. Sci., 50(1), 183-204.

Cook, K. L., Rekapalli, R., Dietze, M., Pilz, M., Cesca, S., Rao, N. P. et al., 2021. Detection and potential early warning of catastrophic flow events with regional seismic networks. Science, 374(6563), 87-92.

Díaz, J., Ruíz, M., Crescentini, L., Amoruso, A. and Gallart, J., 2014. Seismic monitoring of an Alpine mountain river. J. Geophys. Res., Solid Earth, 119(4), 3276-3289.

Hürlimann, M., Coviello, V., Bel, C., Guo, X., Berti, M., Graf, C., Yin, H.Y. et al., 2019. Debris-flow monitoring and warning: Review and examples. Earth-Science Rev., 199, 102981.

Novosad, S., Blaha, P. and Kneijzlik, J., 1977. Geoacoustic methods in the slope stability investigation. Bull. Engineering Geol. and the Environ., 16(1). 229-231

Rao, N. P., Rekapalli, R., Srinagesh, D., Tiwari, V. M., Hovius, N., Cook, K. L. and Dietze, M., 2021. Seismological rockslide warnings in the Himalaya. Science, 372(6539), 247-247.

Rekapalli, R., Yezarla, M. and Rao, N. P., 2024. Discriminating landslide waveforms in continuous seismic data using power spectral density analysis. Geophy. Res. Lett., 51(21), e2024GL110466.

Suriñach, E., Vilajosana, I., Khazaradze, G., Biescas, B., Furdada, G. and Vilaplana, J.M., 2005. Seismic detection and characterization of landslides and other mass movements. Natural Hazards and Earth Syst. Sci., 5(6), 791-798.

Received on: 07-03-2025 ; Revised on: 24-09-2025; Accepted on: 27-09-2025